7th International Conference on Water Resources and Arid Environments (ICWRAE 7): 286-296
4-6 December 2016, Riyadh, Saudi Arabia

Ground Water Exploration and Mapping the Seawater Intrusion at Matruh Area, North Coast, Egypt

[1]El-Said A. AL-Sayed, [1]Gad El-Qady, [1]Nagy Soliman and [2]Abeer El-Kenawy

[1]National Research Institute of Astronomy and Geophysics, 11722 Helwan, Cairo, Egypt
[2]Geology Department, Faculty of Science, Zagazig University, Zagazig, Egypt

Abstract: Matruh area is one of the most promising places for new development projects in the northern coast of Egypt. In despite of the fact that, one of the main development aids is the groundwater resources in the area, these resources are affected by salt-water intrusion from the Mediterranean Sea. In this work, a geoelectrical survey compromised 18 vertical electrical soundings was conducted to investigate and delineate the groundwater aquifer and seawater intrusion in the area. The current electrodes separations (AB) varying from 2 m up to 1000 m in successive steps. To overcome the near surface inhomogeneties (NSIs) and the noisy behavior of the field data, a smoothing algorithm called MEDIAN was applied to the field data. Qualitatively, the iso-resistivity maps were constructed and least squares polynomial separation technique was applied onto the resistivity maps to obtain local resistivity zoning maps, which indicate the seawater intrusion. These maps show that the seawater invaded the study area in north-western and south-eastern parts while the central part is barren from salt water. Eight geoelectrical cross sections portrayed the study area using 1-D inversion results for the VES data. These sections elucidate the subsurface geoelectric situation in the area and show that the shallow section is composed of 4 to 5 geoelectric units, the bottom-mostly layer is fractured limestone having mostly high resistivity. As discerned from the VES study, the groundwater is found mainly in 1 confined fracture zones forming an unconfined aquifer system, which significantly corresponds to the available geological and hydrogeological information.

Key words: Seawater intrusion · DC resistivity · Mars Matruh · Egypt

INTRODUCTION

During the last decade, the Egyptian government made big efforts to develop the northern cost area, which extends westward from Alexandria along the Mediterranean Sea. Many development projects started already, especially those of agricultural and touristic interests. However, there are some environmental problems which hinder this development. Among these problems, seawater intrusion represents the biggest obstacle in either agriculture or obtaining a fresh ground water. The area of study is a part of the eastern side of Matruh area, which is characterized by some faults trending NE-SW and NS along the coastal plain (Fig. 1). The seawater intrudes into the shallow aquifer and contaminates the freshwater.

Geophysics, especially geoelectric techniques have been successfully used to detect the fresh -water/salt-water interface in coastal aquifers [1]. Resistivity surveys are often used to search for ground water in both porous and fissured media. The method provides detailed information about the geometry, source and amount of contamination [2]. Both the apparent resistivity values [3] and the inverted resistivity values [4] can be used for such purposes. Clean sands and gravels, which have high porosities, make good aquifers; when saturated with fresh water they can easily be differentiated from lower-resistivity impermeable clays and marls and also from bedrocks, which is usually distinguished with higher resistivity. In areas where the ground water is significantly saline, the aquifer resistivity is reduced considerably and resistivity method can delineate the boundaries of the body of saline water. Griffith and Barker (1993) [5] present the results of strong resistivity contrast, which can occur across the junction between fresh and saline water using the resistivity survey.

Corresponding Author: El-Said A. AL-Sayed, National Research Institute of Astronomy and Geophysics, 11722 Helwan, Cairo, Egypt.

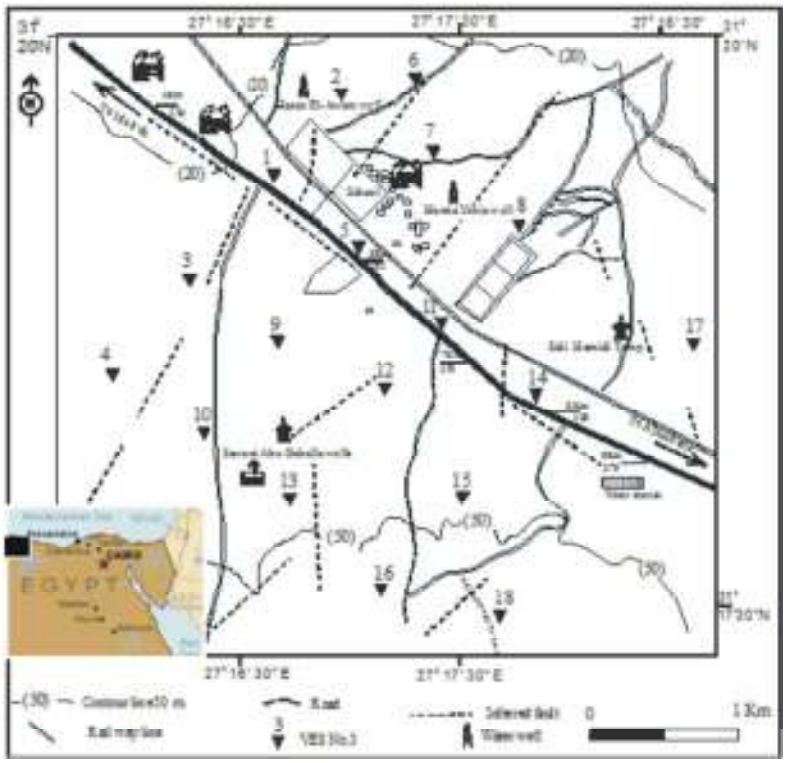

Fig. 1: Location map of the resistivity survey at Matruh area.

Additionally, large differences between the resistivity of saltwater saturated zones and freshwater saturated zones have been used by a number of investigators for determination of saltwater intrusion in many coastal areas [6].

The study area is located between latitudes of 27^0 15' and 27^0 18' E and longitude of 31^0 17' 30" to 31^0 20' N at the 5 Km along Matruh- Alexandria road (Fig.1). This work represents an attempt to study the subsurface structural setting and delineate the ground water aquifer in Matruh area, as well as mapping the seawater intrusion in the fresh water aquifer is performed.

Geological and Hydrogeological Setting: Mersa Matruh area occupies a limited portion of the sub-arid belt dominating the western Mediterranean littoral. It is characterized by very low relief, rarely exceeding 100 m and mild topography. This area is distinguished with two different topographic features, as shown in Fig. (2), the northern coastal plain and the southern tableland [7]. (a) The Northern coastal plain runs almost parallel to the Mediterranean coast. It extends in east –west direction for some 30 Km and has width from north to south of about 8 km, diminishing gradually westwards. This plain displays all signs of a typical emergent coast and is bounded on the southern side by a low sea cliff of Miocene rocks. The landscape in this plain is affected by a number of elongated ridges, which run sub- parallel to the Mediterranean coast. These bids are built of cross-bedded oolitic limestone.

Matruh tableland area constitutes a portion of the arid and sub-arid belt which dominates the southern Mediterranean region where the annual rainfall rarely exceeds 150 mm. It has an elevation varying between 80 and 110 m above sea level and rises some 50 m above the northern coastal plain. It occupies the northern extremity of the Marmarica homoclinal plateau and extends to Qattara Depression. The surface of the tableland area is essentially occupied by calcareous rock composed of alternating beds of limestone and clays with occasional sandstones. El-Shazly and Shata, (1969) [7], have more details about the geomorphologic classification of the northern part of the Western desert.

The geologic succession in the area of study and its surroundings has been studied by [8]; [9]; [10] and [11]. The stratigraphic succession of Matruh area is summarized after [12] (Fig.3). It is totally made of sedimentary rocks belongs to the period from Quaternary to Cretaceous.

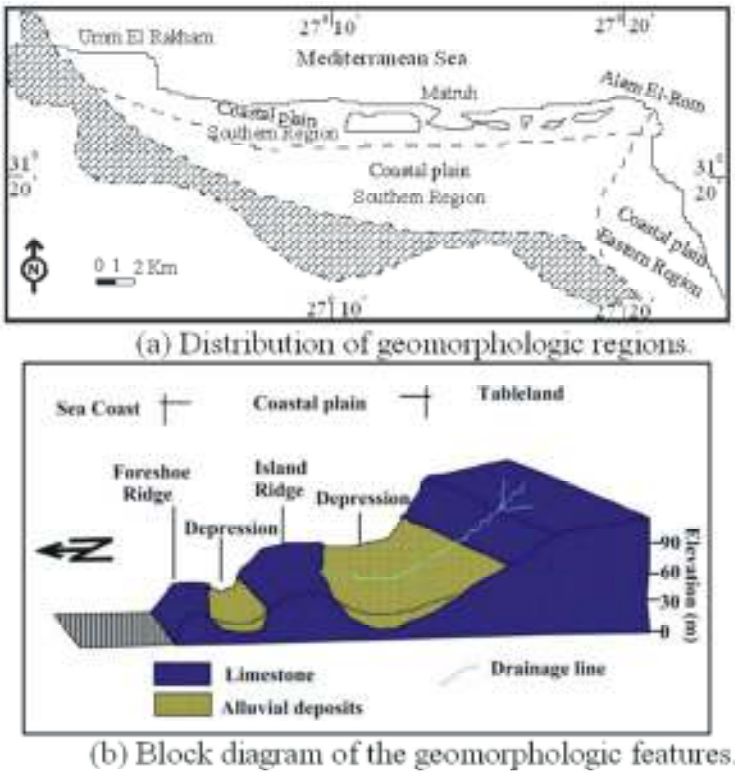

Fig. 2: The generalized geomorphologic regime of Matruh area.

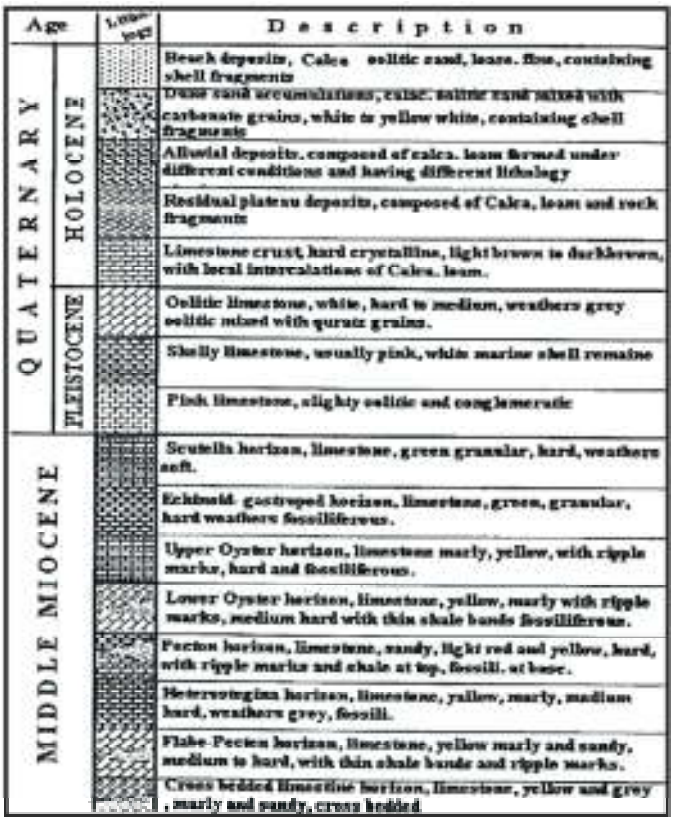

Fig. 3: Summarized geological column for Matruh area and its surroundings.

The quaternary rocks are represented by sand dune accumulations with thickness up to 15 m, followed by calcareous loamy deposits about 10 m thick filling elongated depressions, oolitic limestone about 75 m thick forming the elongated transverse ridges and offshore islands beside the cardium limestone which covers the piedmont plain. In Mersa Matruh area, a subsurface Pliocene section of 43 m thick has been recorded [13]. It composed of two beds, the upper one of creamy limestone of about 26 m, while the lower bed of brown sandstone of about 17 m thick. The Tertiary rocks are represented by pink limestone with a maximum thickness of 125 m at Wadi Abu Gurf and the fossiliferous limestone (Marmarica limestone of Miocene) alternating with sandstone and clay beds. The Eocene rocks are following the younger Tertiary with local unconformities. The Eocene rocks are consisting of carbonates with interbedded shale. Eocene rocks overlap late Cretaceous rocks, which consist of a thick section (520 to 1080 m) of marine limestone, dolomite and chalk. However, the tectonic movements cause uplift and differential erosion of the upper cretaceous [14].

Structurally, Matruh basin is a north-trending intracratonic, taphrogenic structure. It is suggested that the initial graben is a failed arm of a late Triassic or early Jurassic crustal rift, possible related to rifting and seafloor spreading between turkey and North Africa [9]. Shata (1955) [8] suggested that the E-W topographic features in Matruh area resulted from gentle epoirogenetic movement that took place during post Miocene time. These features are represented by a series of normal faults, which affected the Miocene limestone producing the structural plateau of the tab land (Fig.1). A series of NE-SW monoclinal structure was recorded along the coast strip. These structural features affected Groundwater conditions in the area [8]. The water bearing formations in several localities are controlled by some faults, which take E-W and NW-SE trends.

Geophysical Data: The geophysical study conducted in this work concerns with a DC resistivity survey utilizing the well-known Schlumberger array. Eighteen vertical electrical soundings (VESes) were measured as shown in Fig. (1) with current electrode separation (AB) varying from 2 m up to 1000 m in successive steps. The increase of potential electrode spacing is often marked by a discontinuity in the field curve. At the discontinuities, we repeated the measurements, then the field curves are smoothed before digitization.

Data Processing and Interpretation: The DC resistivity field data are inherently noisy. This noisy behavior could be due to the near surface inhomogeneties (NSI's) and/or deep seated geological inhomogeneties. Distortion of VES curve caused by such objects may be divided into two main types. The first one is caused by objects near to potential electrodes, which is called P-effect, while the other one caused by objects near to current electrodes and is called C-effect. An algorithm MEDIAN, [15], was used to filter the field data measured in this work, which enables to remove NSI's. Fig. (4) shows a correlation of some VES curves before and after the filtering. Fig. (5) shows the comparison between general iso-apparent resistivity sections containing all VESes before and after filtering using the Median algorithm.

Qualitative Interpretation: The qualitative interpretation in this work is represented by the iso-apparent resistivity maps. Five iso-apparent resistivity maps are constructed at AB/2=10, 30, 60, 200 and 400 m, shown in Figs. 6,7,8,9 and 10, respectively. The interpretation of iso-apparent resistivity maps is difficult because apparent resistivity data not only depends on geoelectric subsurface structures but also on the used electrode array. To somewhat the fictitious nature of the interpretation of apparent resistivity data is sometimes ambiguous [3]. For these difficulties, a least-squares polynomial technique [16], which is issued in gravity and magnetic field data is used to separate the field data into regional (REG) and residual (RES) components [17].

The regional resistivity pattern is removed to emphasize the local effects of seawater invasion on the shallow subsurface section. The iso-apparent resistivity maps show the general subsurface situation and the local resistivity maps will reflect the local variations in resistivity values and represent the local subsurface geological influences. The local resistivity maps were reduced only to the zero contours in order to obtain the resistivity zoning maps. These local resistivity-zoning maps are able to differentiate between negative and positive zones. Negative resistivity zones are due to the invasion of seawater on the surface and shallow subsurface layers, while positive zones may be attributed to dry and/or compact sediments in the surface layers and to hard rocks in the subsurface. Although the zero iso-residual lines may not necessarily coincide with geological boundaries, they certainly do approximately outline areas of similar geoelectrical properties.

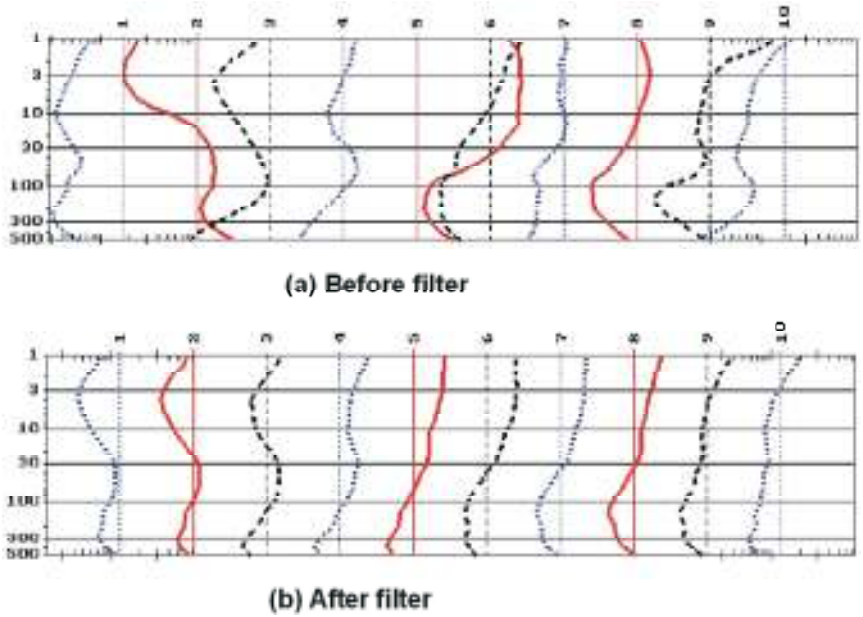

Fig. 4: Correlation of VES's curves before and after filtering.

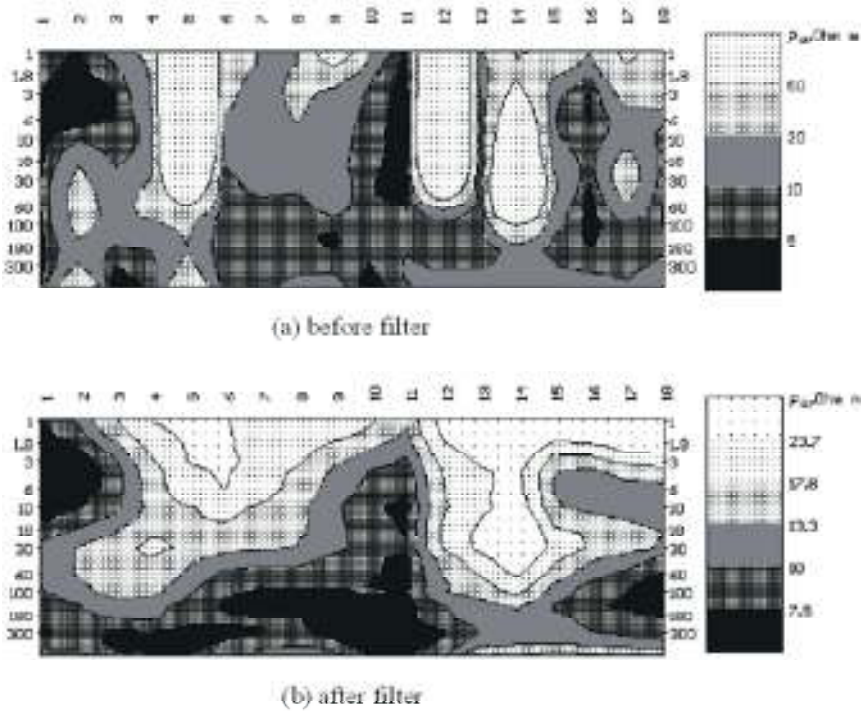

Fig. 5: Comparison between general Iso-apparent resistivity section before and after filter.

From the qualitative interpretation of these maps (Figures 6, 7, 8, 9 and 10) we can noticed that the apparent resistivity values decrease with increasing depth, which reflect the increasing of the conducting materials with depth. The residual resistivity component is obtained using the least squares method in order to delineate the effects of seawater on the subsurface.

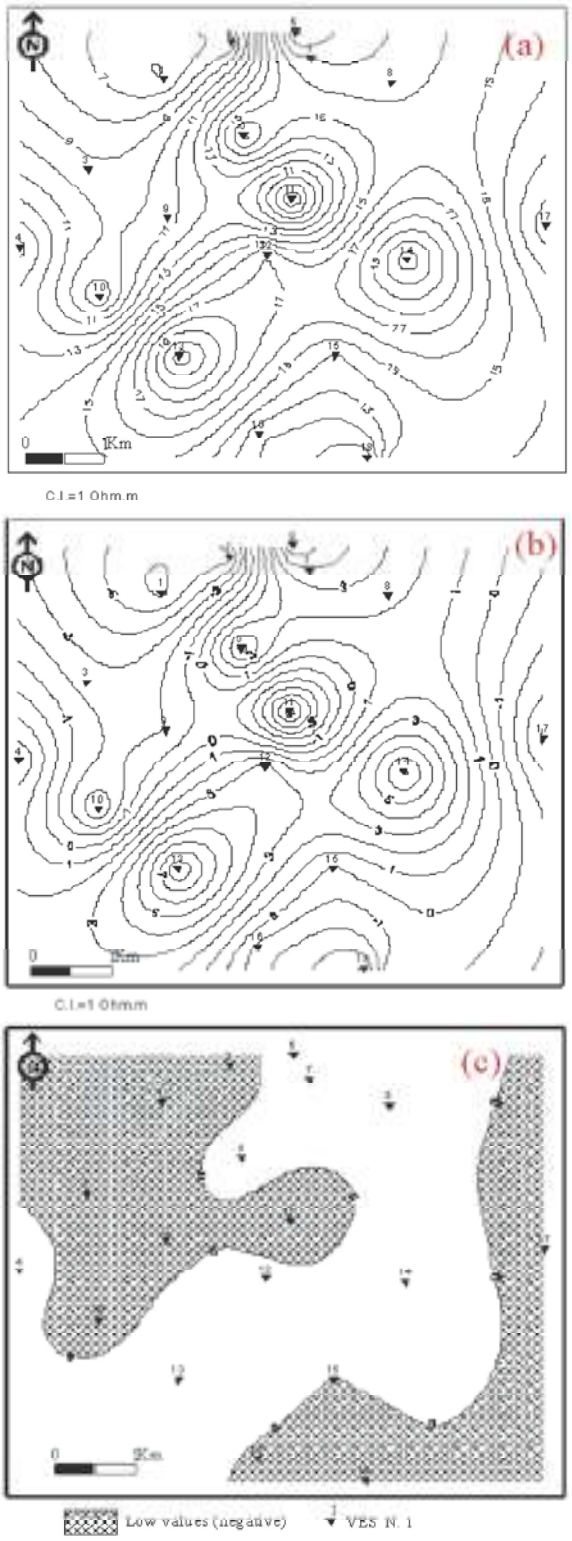

Fig. 6: Iso-resistivity maps at AB/2 = 10 m.
(a) Iso-apparent resistivity, (b) Residual map and
(c) Zoning resistivity map

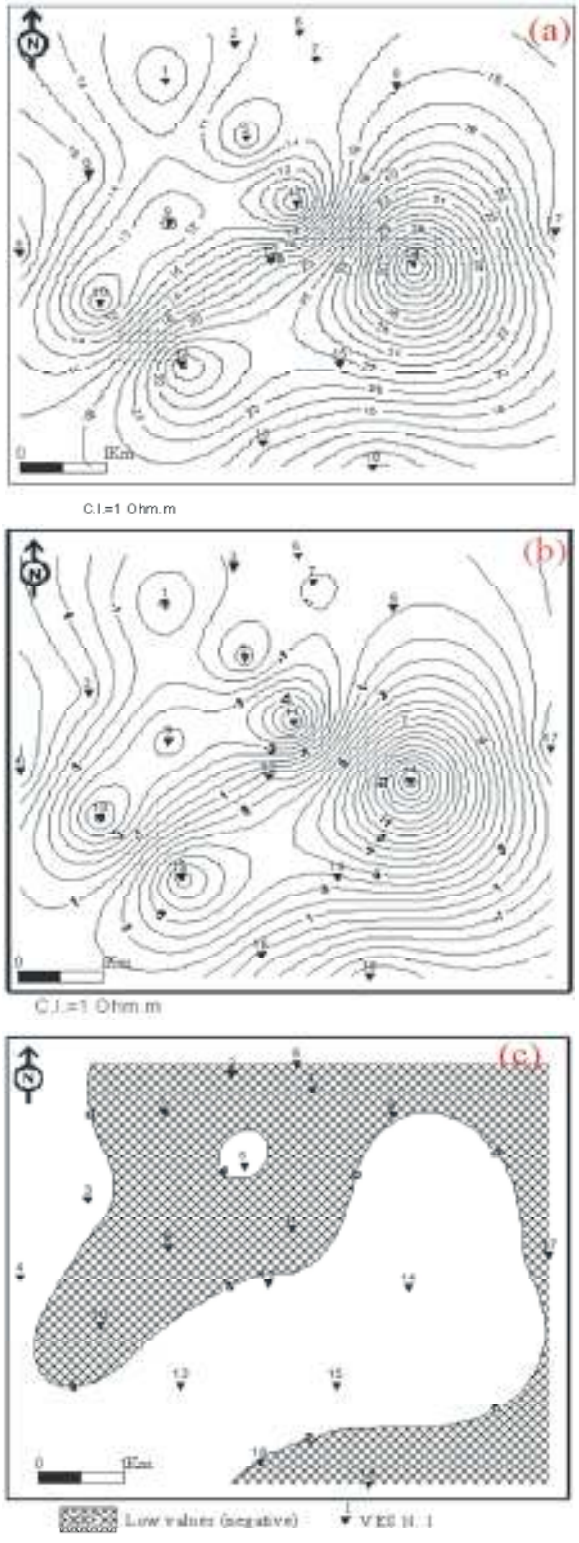

Fig. 7: Iso-resistivity maps at AB/2 = 30 m.
(a) Iso-apparent resistivity, (b) Residual map and
(c) Zoning resistivity map

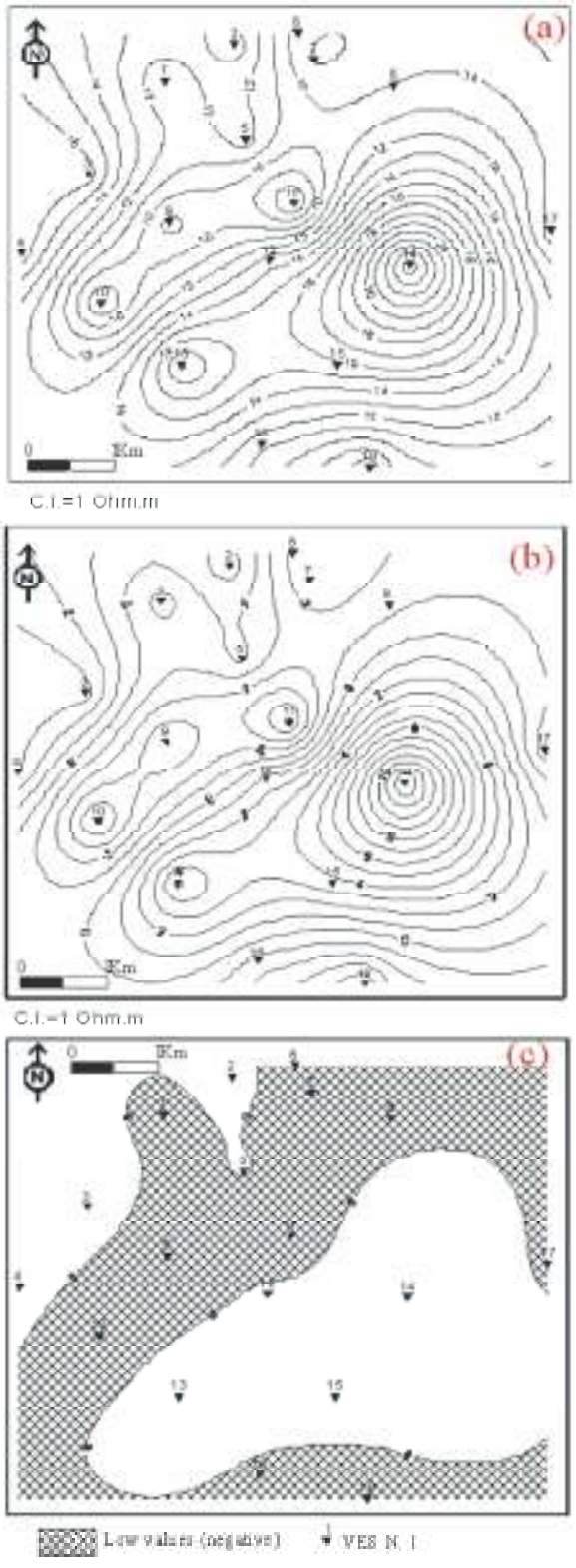

Fig. 8: Iso-resistivity maps at AB/2 = 60 m. (a)Iso-apparent resistivity, (b) Residual map and (c) Zoning resistivity map

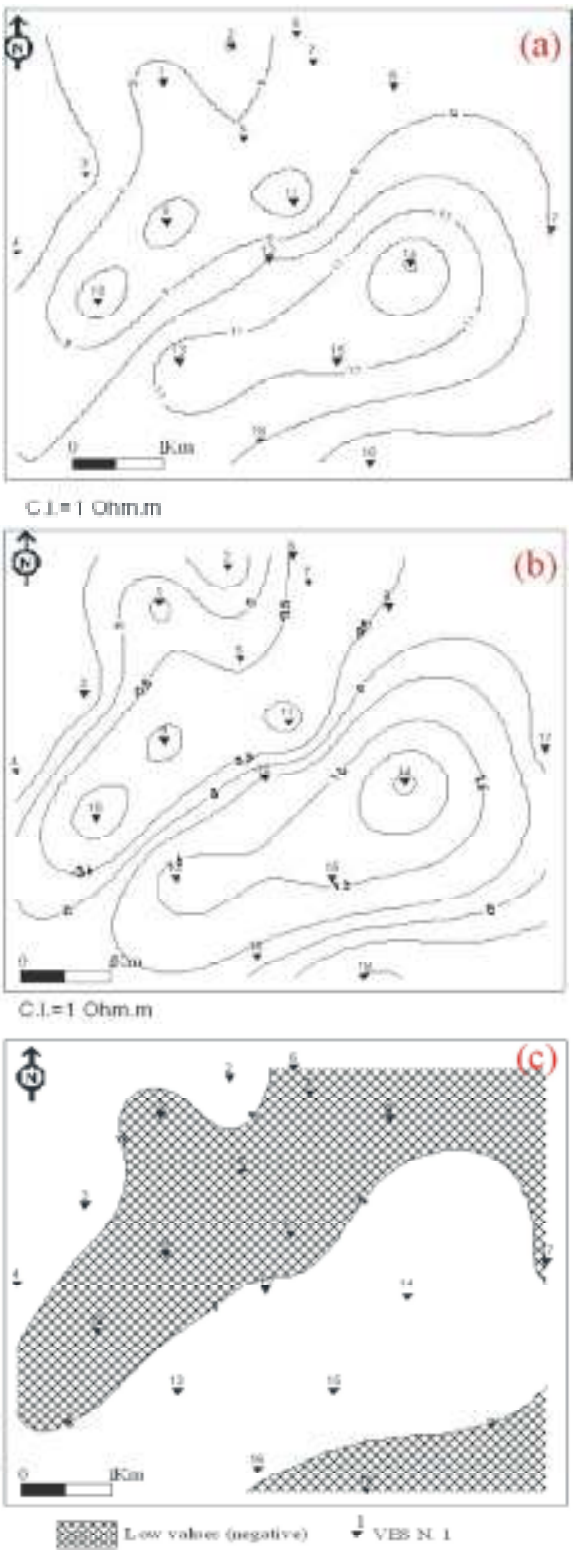

Fig. 9: Iso-resistivity maps at AB/2 = 200 m. (a) Iso-apparent resistivity, (b) Residual map and (c) Zoning resistivity map

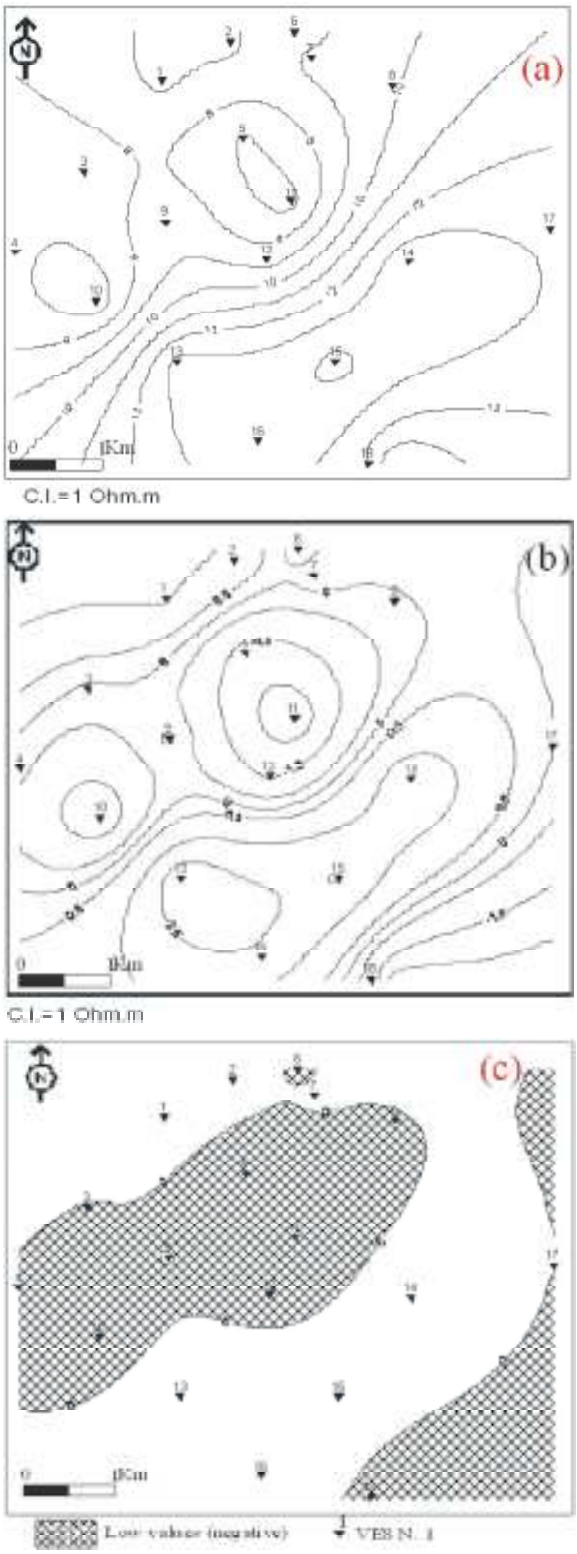

Fig. 10: Iso-resistivity maps at AB/2 = 400 m.
(a)Iso-apparent resistivity, (b) Residual map and (c) Zoning resistivity map.

Additionally, we can conclude that the seawater intrusion is increasing at the north- western and south-eastern parts of the area of study with different degrees of depth. The central part of the area is nearly avoided from the salt-water intrusion.

Quantitative Interpretation: Due to the problem of non-uniqueness of the resistivity data interpretation, we have experimented the filtered data with two programs for 1-D interpretation of resistivity data [18] and [19]. In both cases, theoretical curve is calculated or initial model is introduced, the process goes iteratively until a good match between the observed and the theoretical curve is found. The inversion results for all the 18 VES points are interpreted and subsequently correlated to resolve the lithological condition in the study area. The nature and distribution of different lithological layers are represented by the geoelectric cross sections.

The Geoelectric Cross-Sections: Eight geoelectric cross-sections are portrayed across the area of study, some of them have the SW-NE direction and others have NW-SE direction. These sections elucidate the subsurface geoelectric layers and the extension of the groundwater aquifer in the area of study. These cross-sections show that the shallow subsurface section is composed of 4 to 5 geoelectric layers.

The geoelectric cross-section A-A` goes through the VES numbers 4, 3, 2, 1 and 6 respectively. It is composed of five geoelectric layers as shown in Fig. (11). The surface alluvium deposits cover the surface of the study area with a relatively moderate resistivity values. Sometimes these deposits change to fine silt and clay materials (e.g. at VES 2, 1 and 6). This layer is followed by a relatively low resistivity unit representing the upper shale layer. This layer disappears at VES No.3, probably as a result of the inferred fault between soundings No. 3 and 2. Following upper shale layer, there is a unit of moderate resistivity values range between 8 and 69 Ohm.m with thickness varying from 20 to 120 m. This unit represents the oolitic limestone, sometimes marly, which is considered as the shallow water aquifer in the area and correlates well with the available information derived from the nearby water wells. This unit is followed by a relatively thick low resistivity unit with a resistivity value ranges between 2 and 6 Ohm.m. It represents the lower marl and clay layer. Due to the inferred fault between the soundings No. 3 and 2, we find this unit

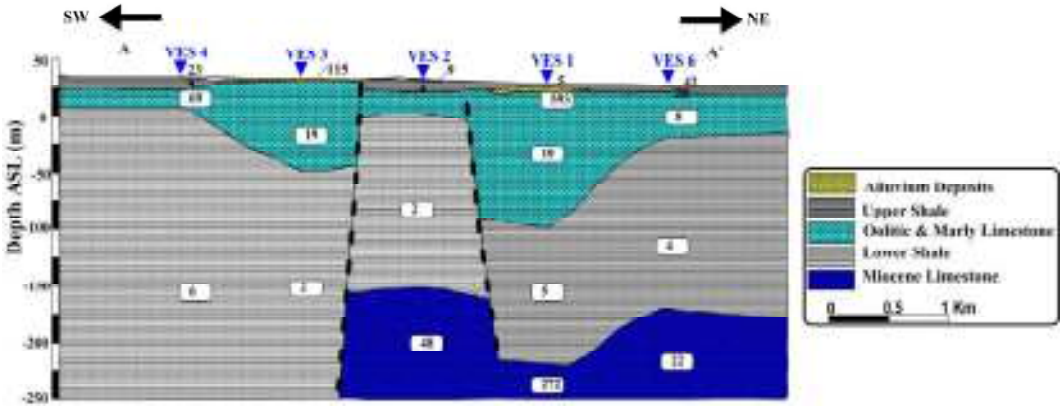

Fig. 11: The Geoelectrical cross-section A-A`.

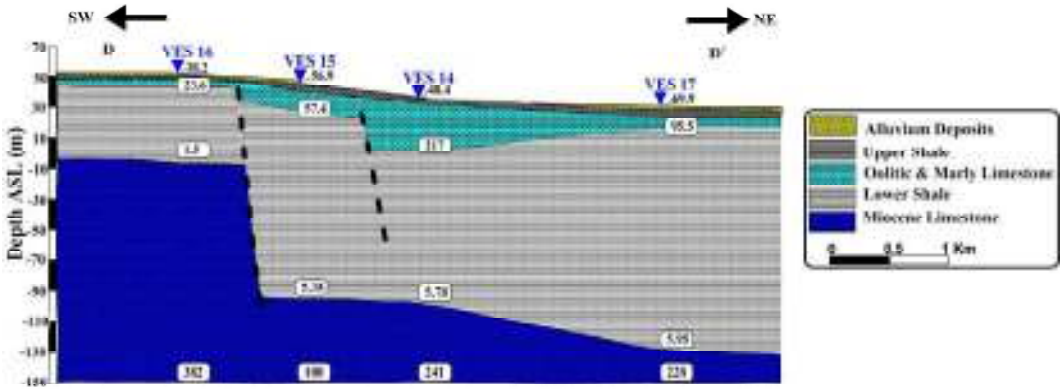

Fig. 12: The Geoelectrical cross-section D-D`.

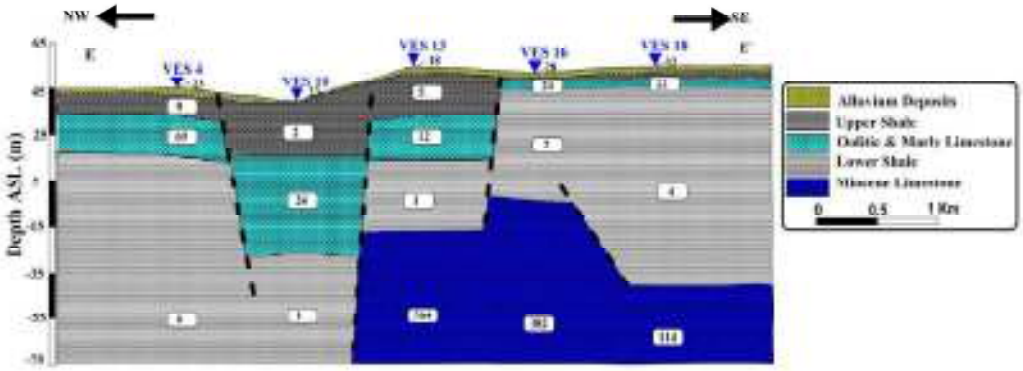

Fig. 13: The Geoelectrical cross-section E-E`.

extends to the base of the investigated section, while a relatively high resistivity unit following the shale layer extends to the end of the section. This unit represents the fissured limestone of Middle Eocene and is considered as the deepest aquifer in the area.

Far to the South of the study area, the geoelectric cross-section D-D` (Fig. 12) is composed of the same geoelectric units representing alluvium deposits, upper shale, oolitic limestone, lower shale and limestone layer from top to bottom respectively. However, due to the inferred faults between soundings No. 16 and 15 then between 15 and 14, we find a big variation in the thickness of the lower shale layer along the section. Accordingly, a major uplift for the fracture limestone, deep aquifer, at the VES No. 16 is attained.

In the geoelectric cross-section E-E` (Fig. 13), there are series of faults composing graben-horst structures. These kinds of faults make discontinuities in the shallow oolitic limestone aquifer; even they control the thickness of the aquifer itself, giving a maximum thickness of about 40 m at VES No. 10. Meanwhile, we couldn't reach the deepest aquifer at both soundings No. 4 and 10.

CONCLUSION

This study aims to outline the hydrogeological conditions in Matruh area depending on the geoelectric resistivity survey, in addition, to map the seawater intrusion in the area. The geoelectric investigation coupled with the geological and hydrogeological information reveals the following characteristics of Matruh area, in relation to geological setting and aquifer conditions:

- The area of investigation consists of 4 to 5 prominent lithologic layers; the bottom mostly layer is fractured limestone having mostly high resistivity. Groundwater, in mainly confined fracture zones; forms an unconfined aquifer system. The groundwater conditions of the area, as discerned from the VES study significantly correspond with the available geological information as well the information derived from the nearby water wells.
- The seawater invades the study area mostly at north-western and south-eastern parts at different depths, while the central parts almost are avoided from the seawater intrusion. This could be due to the fault system, which controls the groundwater flow direction.
- Series of faults dissecting the area in different directions sometimes compose graben–horst structures. These faults make a discontinuity in the groundwater bearing formation; consequently they control the seawater intrusion in the study area, so that the central part of the studied area is almost avoided from the seawater invasion.

ACKNOWLEDGMENT

We are indebted to all the staff of the National Research Institute of Astronomy and Geophysics (NRIAG) for acquiring the resistivity data.

REFERENCES

1. Barker, R.D., 1980. Application of Geophysics in groundwater investigations. Water Surv., 84: 489-492.
2. Kelly, W., 1976. Geoelectric sounding for delineating groundwater contamination. Ground Water, 14: 6-10.
3. Benson, A., K., Payne and M. Stubben, 1997. Mapping groundwater contamination using D.C resistivity and VLF geophysical methods-A case study. Geophysics, 62: 80- 86.
4. Töpfer, K.D., 1976. Representation and interpretation of resistivity mapping data in groundwater prospecting in Zambia. J. Geophys, 42: 147-158.
5. Griffiths, D.H. and Barker, 1993. Two-dimensional resistivity imaging and modeling in areas of complex geology. J. Appl. Geophysics, 29: 211-226.
6. Frohlich, R.K., D. Urish, J. Fuller and M.O. Reilly, 1994. Use of geoelectrical methods in groundwater pollution surveys in a coastal environment. J. Applied Geophysics, 32: 139-154.
7. El-Shazly, M. and A. Shata, 1969. Geomorphology and Pedology of Mersa Matroh area, western Mediterranean Littoral zone. Bull. Inst. Desert, Egypt, 19(1): 1-30.
8. Shata, A., 1955. An introduction note on the geology of the northern portion of the Western desert of Egypt. Bull. Inst. Desert Egypt, Vol. 5, No.3.
9. Prior, S.W., 1976. Matruh basin, possible failed arm of Mesozoic crustal rift. 5th Explor. Seminar, Egypt. Gen. Pet. Corp., Cairo, pp: 11.
10. Hammad, F., A. Taha and A. Shata, 1986. Study of landforms in the area between Ras El Hekma and Ras Alam ElRum, North western Mediterranean littoral zone, Egypt. Mansoura Sc. Bull., Fac. Sc. Mansoura Univ., 13(1): 189-210.
11. Hantar, G., 1990: North Western Desert. In: Geology of Egypt, ch.15, Ed. Said, R. 1990.
12. El Senussi, M.Y. and A.A. Shata, 1969. The stratigraphy of Umm El Rakham area. Bull. Inst. Desert, Egypt. 19(2): 1-32.
13. El-Shazly, M.M., 1964. Geology, Pedology and hydrogeology of Mersa Matruh area. Unpublished Ph. D thesis, Fac. Sci. Cairo Univ.
14. Said, R., 1962: The geology of Egypt. Elsevier Publ. Amsterdam, pp: 377.

15. Modin, I., V. Shevnin, E. Pervago, A. Bobatchev, M. Marchenko and A. Lubchikova, 1994. Distortion of VES data caused by subsurface inhomogeneities. Proc. of EAEG 56th annual meeting, Austria, June 6-10, pp: 129.
16. Agocs, W., 1951. Least squares residual anomaly determination. Geophysics, 4: 686-696.
17. Nettleton, L.L., 1954. Regional, residual and structures. Geophysics, 19: 1-22.
18. Bobachev, A., I. Modin, E. Prevago and V. Shevnin, 1990. IPI-1D program set for 1D data interpretation, Russia, Moscow State University, Geological Faculty, Dept of Geophysics.
19. Zohdy, A., 1989: Anew method for the automatic interpretation of Schlumberger and Wenner sounding curves. Geophysics, 54(2): 245-253.